J Vet Intern Med 2014;28:799–808

In Vivo Histologically Equivalent Evaluation of Gastric Mucosal Topologic Morphology in Dogs By using Confocal Endomicroscopy

M.J. Sharman, B. Bacci, T. Whittem, and C.S. Mansfield

Background: Confocal endomicroscopy (CEM) is an endoscopic technology permitting in vivo cellular and subcellular imaging. CEM aids real-time clinical assessment and diagnosis of various gastrointestinal diseases in people. CEM allows in vivo characterization of small intestinal mucosal morphology in dogs.

Objective: To determine the feasibility of CEM to evaluate gastric mucosal morphology in dogs and to characterize the appearance in healthy dogs.

Animals: Fourteen clinically healthy research colony dogs.

Methods: Experimental study. Under general anesthesia, dogs underwent standard endoscopic evaluation and CEM of the gastric mucosa. In the initial 6 dogs, fluorescent contrast was provided with the fluorophore acriflavine (0.05% solution), applied topically. Subsequently, 8 dogs were assessed using a combination of fluorescein (10% solution, 15 mg/kg IV), followed by acriflavine administered topically. For each fluorophore, a minimum of 5 sites were assessed.

Results: Confocal endomicroscopy provided high quality in vivo histologically equivalent images of the gastric mucosa, but reduced flexibility of the endoscope tip limited imaging of the cranial stomach in some dogs. Intravenous administration of fluorescein allowed assessment of cellular cytoplasmic and microvasculature features. Topical application of acriflavine preferentially stained cellular nucleic acids, allowing additional evaluation of nuclear morphology. Identification of *Helicobacter*-like organisms was possible in 13 dogs.

Conclusion and Clinical Importance: Confocal endomicroscopy provides in vivo images allowing assessment of gastric mucosal morphology during endoscopy, potentially permitting real-time diagnosis of gastrointestinal disease.

Key words: Acriflavine; Endoscopy; Fluorescein; Gastroenterology; Gastrointestinal.

Confocal endomicroscopy (CEM) is an endoscopic technique permitting simultaneous wide-field view of video endoscopy and real-time microscopic imaging of the gastrointestinal mucosa.[1–4] CEM is achieved either by integration of a miniaturized confocal microscope into a conventional flexible endoscope, or by the use of confocal miniprobes passed through the biopsy channel of a conventional video endoscope.[1,4–6] Intravenous or topically administered exogenous fluorophores provide contrast to allow acquisition of confocal images which provide cellular and subcellular detail.[1,5,6] Histopathologically equivalent "virtual biopsies" can therefore be obtained during endoscopic procedures, potentially providing in vivo diagnostic capability.[7–9]

In people, CEM has been evaluated for clinical assessment of a range of gastrointestinal pathologies and is a routine diagnostic procedure in some practices.[1,3,8,10–13] The feasibility of CEM to evaluate and describe normal small intestinal mucosal epithelial and vascular morphology in dogs, as well as its capacity to identify and evaluate the spatial location of *Helicobacter*-like organisms (HLOs), has previously been reported by the authors.[14,15]

The aim of this study was to evaluate the feasibility of CEM for evaluation of the gastric mucosa by using topical and intravenous exogenous fluorophore protocols currently utilized in people and to evaluate and describe normal gastric mucosal topologic morphology in clinically healthy dogs.

Abbreviations:

CEM	confocal endomicroscopy
FITC	fluorescein isothiocyanate
RBCs	red blood cells
WLE	white light endoscopy
WSAVA	World Small Animal Veterinary Association

Materials and Methods

Animals

Fourteen healthy adult mix-breed research colony dogs (10M, 4F) with no observed gastrointestinal clinical signs were studied. Dogs were housed within the University of Melbourne's dog colony, and were considered healthy before inclusion based on physical examination, routine hematology, and serum biochemistry. Vaccinations and parasite prophylaxis were current for all dogs. The University of Melbourne's Animal Ethics Committee approved all dog use according to National Health and Medical Research Council guidelines (Animal Ethics Committee [AEC] numbers 1112209 and 1112075).

Equipment

Endoscopic procedures were performed using one of 3 prototype confocal endomicroscopes developed by integration of a miniaturized confocal microscope into a standard video endoscope

From Translational Research and Animal Clinical Trial Study (TRACTS) Group, the Faculty of Veterinary Science, The University of Melbourne, Melbourne, Vic., Australia (Sharman, Bacci, Whittem, Mansfield).

Corresponding author: M.J. Sharman and C.S. Mansfield, Faculty of Veterinary Science, The University of Melbourne, 250 Princes Highway, Werribee, Vic. 3030, Australia;
e-mails: melloras@unimelb.edu.au and cmans@unimelb.edu.au.

Submitted August 29, 2013; Revised January 6, 2014; Accepted January 21, 2014.

DOI: 10.1111/jvim.12332

(Olympus, GIF-Q145 and Olympus PCF-Q180AI)[a] by Optiscan Imaging.[b] For confocal imaging with either of the endomicroscopes, a solid state laser, with a variable power output (0–1,000 μW), delivered 488 nm (blue) laser light via a single optical fiber capable of focusing to a single, diffraction limited plane within the tissue. Fluorescence in the range of 405–590 nm wavelengths was detectable. Image depth could be varied up to 250 μm, at ~3 μm increments with acquisition of images throughout this depth range (*z*-axis). This allowed sampling of a 3-dimensional volume equivalent to an "optical biopsy." Axial (7 μm) and lateral (0.5 μm) resolution permitted evaluation of both cellular and subcellular detail.

Procedure

Dogs were fasted for 12 hours prior to gastroduodenoscopy. Each dog received sedation with acepromazine (0.01 mg/kg IV)[c] and methadone (0.1 mg/kg IV)[d] before induction of anesthesia with alfaxalone (2 mg/kg IV).[e] General anesthesia was maintained with isofluorane[f] in oxygen and all dogs received IV fluid therapy for the duration of the procedure (Hartmann's solution, 10 mL/kg/h).

For all dogs, gross morphologic assessment of the gastric mucosa by using standard white light endoscopy (WLE) was first performed, followed by administration of exogenous fluorophores to provide sufficient fluorescent contrast for CEM to be accomplished. For all procedures, evaluation of each gastric region (pyloric antrum, gastric body, cardia, and fundus) was attempted for each endoscopic modality. In the initial 6 dogs evaluated with the Olympus GIF-Q145 endoscope, the exogenous fluorophore acriflavine was used alone and was applied topically (30–90 mL of 0.05% aqueous solution)[g] to the gastric mucosal surface via the use of an endoscopy washing catheter (Olympus, PW-2L-1).[h] In the remaining 8 dogs evaluated with the Olympus PCF-Q180AI endoscope, the exogenous fluorophore fluorescein (15 mg/kg; 10% aqueous solution)[g] was first administered as an IV bolus injection as previously described.[6,14] Once assessment with fluorescein was complete, acriflavine was then applied topically, as above.

Confocal endomicroscopy was performed by placing the tip of the endoscope containing the confocal microscope in direct contact with, and en face to the mucosal surface as previously described by the authors.[6,14,15] A minimum of 5 sites were assessed for each fluorophore, encompassing each gastric region where possible. At each location "optical biopsies" were obtained by sequentially adjusting the *z*-axis by 3–6 μm intervals until resolution and contrast were insufficient for adequate image interpretation. Images were obtained at a variety of frame rates and resolutions ranging from 0.8 frames/s (at 2.1 megapixels) to 6 frames/s (at 0.25 megapixels). Both *z*-axis adjustment and image acquisition were controlled with a foot pedal.

Multiple endoscopic pinch biopsy specimens (6–8 per dog) were collected from corresponding regions of gastric mucosa and preserved in 10% buffered formalin for histologic comparison. Serial sections (4–5 μm) of paraffin embedded samples were obtained and stained with hematoxylin and eosin (H&E). Samples were sectioned as for standard histologic assessment and, where possible, orthogonal sections were also acquired and evaluated, en face to the mucosal surface, in order to correspond with confocal images. Confocal images were evaluated and described in combination with corresponding, and standard, histopathology images, by 2 authors (BB and MJS). Histopathology standards for the diagnosis of gastrointestinal inflammation, developed by the World Small Animal Veterinary Association Gastrointestinal Standardization Group, were used to interpret histologic sections.[16]

The presence and frequency of CEM image artifacts that interfered with confocal image interpretation were assessed by review of all captured images from each of the initial 6 procedures as these had all been performed by a single user. Procedures were reviewed in a randomized order by 1 author (MJS) and the number of images affected by each artifact was expressed as a percentage of the overall number of images captured.

Results

White Light Endoscopy and CEM Examination

In contrast to the Olympus PCF-Q180AI endoscope, the Olympus GIF-145 endoscope did not allow complete WLE examination of the fundus and cardia by using a standard J-maneuver as integration of the confocal microscope into the tip of the endoscope limited its flexibility. Similarly for CEM, the flexibility of the Olympus GIF-145 endoscope limited evaluation sites primarily to regions within the lower gastric body and pyloric antrum. Images of the cardia and fundus were acquired by modifying the imaging technique so that the endoscope was withdrawn toward the lower esophageal sphincter then angulated and rotated, rather than simply angulated, against the mucosal surface. Improved flexibility of the endoscope tip with the Olympus PCF-Q180AI endoscope allowed all regions of the stomach to be evaluated by using more standard maneuvers. Gross mucosal abnormalities were only detected by WLE in 1 dog. In this dog, the gastric mucosa within the pyloric antrum appeared irregular and erythematous, with regular small superficial ulcerations noted.

Examination of the gastric mucosa by CEM was able to be performed in 13/14 dogs, with acquisition of high quality microscopic images, including cellular and subcellular detail (Figs 1A–D, 2A–D). Images were immediately available and potentially able to be interpreted in real time. In the 1 dog with gross WLE change as described above, marked alteration in mucosal morphology was detected by CEM and subsequently a histopathologic diagnosis of lymphocytic gastritis was made. CEM images from this dog were therefore excluded from further analysis.

Fluorescein provided adequate fluorescent contrast because of redistribution from the vascular space to the interstitial and intracellular spaces within seconds of intravenous administration. Fluorescein was uniformly distributed throughout the mucosa within the stomach providing consistent fluorescent intensity in all gastric regions. Contrast was adequate for a duration of 30 minutes, although diminished in the latter part of this time frame requiring both higher laser power and brightness settings to achieve images of similar resolution. Fluorescence provided by topical application of acriflavine was limited to the region of application, and reapplication was required when an area with inadequate uptake was identified. When adequate distribution of acriflavine was achieved, fluorescent intensity was variable both between dogs as well as within the different regions of the stomach

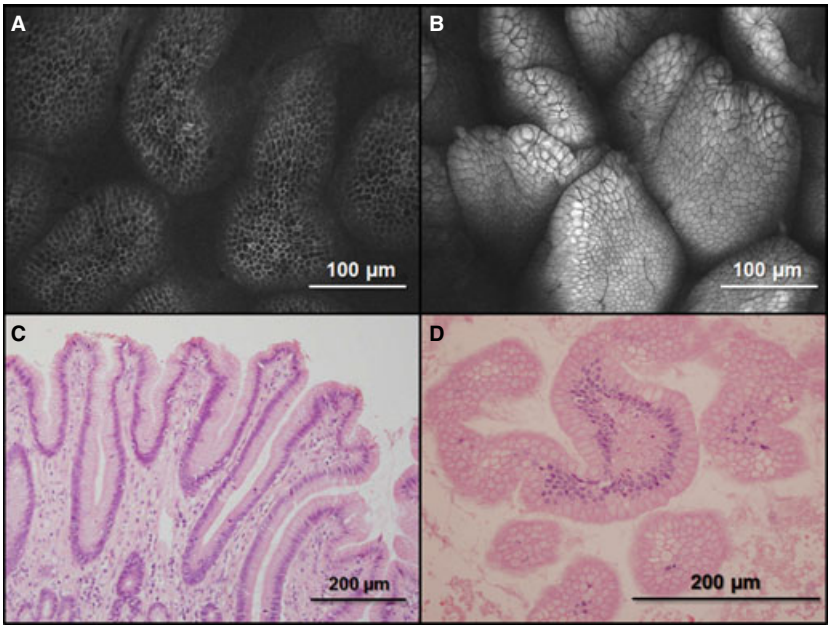

Fig 1. **(A) Pyloric antrum**. Confocal endomicroscopy (CEM) image of the mucosal surface of the lower pyloric antrum. Only cellular cytoplasmic features are highlighted. Superficial imaging of the mucosal surface demonstrates the regular mosaic pattern of the epithelial cells. Image collected after intravenous administration of fluorescein. **(B) Pyloric antrum**. Topical administration of acriflavine results in preferential staining of nuclear contents providing superior visualization of individual cells and enhancing the superficial mosaic pattern. Histologic images of the pyloric antrum, including standard orientations **(C)** and orientations comparative to those obtained by using CEM **(D)** are also shown.

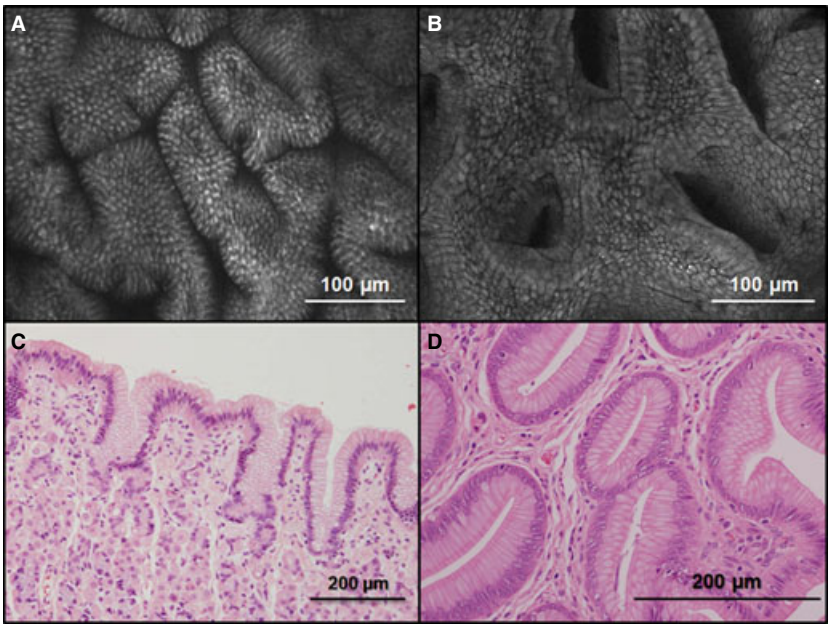

Fig 2. Confocal endomicroscopy (CEM) allowed differences in mucosal morphology corresponding to known histologic differences among the various regions of the stomach to be appreciated with either fluorophore. **(A)** Upper pyloric antrum after intravenous administration of fluorescein. **(B)** Gastric body after topical administration of acriflavine demonstrating a flattened mucosal architecture with round-to-elliptical gastric pit openings separated by wide mucosal folds. Histologic images including standard orientations **(C)** and orientations comparative to those obtained by using CEM **(D)** are also shown.

being examined. The most intense fluorescent contrast was consistently achieved within the pyloric antrum, whereas fluorescent intensity was often quite poor within the gastric body. Where cellular uptake of the exogenous fluorophores was poor, the overall gross morphology and gastric pit pattern could still often

be appreciated due to pooling of the fluorescent agents on the surface of the mucosa and within the gastric pits.

Using either of these fluorophores, epithelial cells formed a regular mosaic pattern at the mucosal surface, and fine, shallow invaginations were frequently seen along the surface (Figs 1A–B, 2A–B). Deeper within the mucosa, the distinction between the surface epithelial cell layer and the lamina propria could be made as individual columnar epithelial cells lined up against the basement membrane (Fig 3A–C). Depending upon the particular fluorophore used, both cellular and subcellular features, including nuclear detail, could be distinguished for cells both within the epithelial layer and lamina propria. With fluorescein, the subsurface microvascular network could also be partially visualized.

Differences in overall mucosal morphology, which corresponded histologically with different regions of the stomach, were also able to be appreciated with both fluorophores (Figs 1, 2A–D). Within the pyloric antrum, elongated gastric pits provided the appearance of villous-like projections from the mucosal surface, with narrow bridging connections, and these were predominantly seen in transverse section, as compared with standard histologic tissue positioning (Fig 1A and B). Higher in the pyloric antrum, gastric pits were seen as elongated, continuous, and branching slits (Fig 2A). In comparison, the shorter gastric pits within the gastric body gave an overall more flattened architecture to the mucosa and pit openings in this region were wider, round to elliptical or diamond shaped at the luminal surface and separated by wide mucosal folds (Fig 2B). Branching of the tubular glands could be followed by sequentially adjusting the *z*-axis to allow collection of images from sequentially deeper sections within the mucosa. Isolated or small clusters of epithelial cells that had been shed into the lumen were occasionally seen and the process of epithelial shedding could, on occasion, be observed in real time (Video S1).

As operator experience improved, an overview of a particular region was more frequently gained by increasing the rate of scanning to allow quick assessment of a larger section of the gastric mucosal surface. If a particular area of interest was identified, scan rate could then be decreased to evaluate high resolution images.

Fluorescein

Fluorescein allowed evaluation of cellular cytoplasmic, but not nuclear features. On the mucosal surface, epithelial cells formed a regular mosaic pattern, with fluorescein especially highlighting the border of individual cells. By adjusting the focal plane to provide a cross-section of the villi within the pyloric antrum, the arrangement of columnar epithelial cells along the basement membrane could be delineated. The dense, subsurface microvascular network was visible just below the epithelial surface; however, the definition of the microvascular network was indistinct and was seen as a diffuse fluorescent intensity within the lamina propria (Fig 4). The passage of individual red blood cells (RBCs) was not readily discernible.[14] By adjustment of the z-axis, imaging with IV fluorescein was useful to a depth of approximately 80–120 μm at which point resolution became insufficient to allow accurate interpretation of cellular detail.

Acriflavine

Preferential nuclear staining was achieved with the topical application of acriflavine, and this provided superior visualization of individual cells both within the lamina propria and the surface epithelial cell layer.

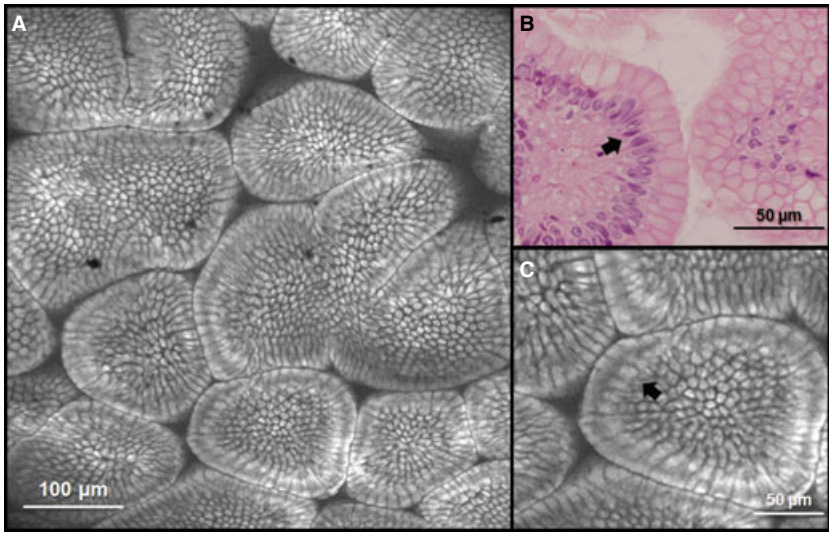

Fig 3. **(A)** Topical administration of acriflavine in combination with subsurface imaging ensures individual cells within the lamina propria are identifiable. **(B, C)** The distinction between the surface epithelial cell layer and the lamina propria is seen where the nuclei of individual columnar epithelial cells line up against the basement membrane (black arrow) and are comparative to that seen histologically (B).

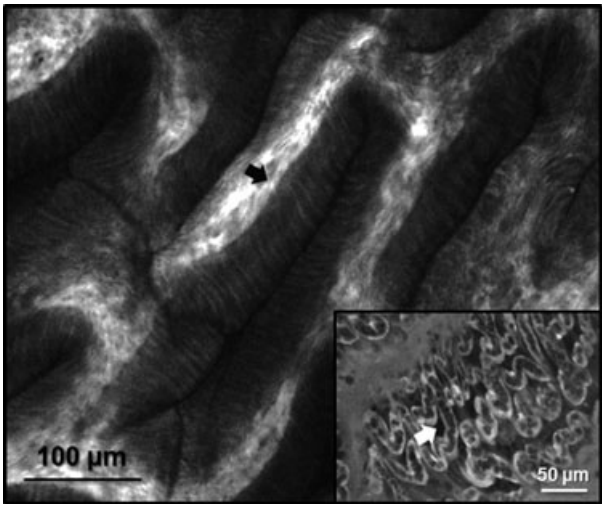

Fig 4. Subsurface imaging after administration of intravenous fluorescein allows the distinction between the superficial epithelial layer and the lamina propria (black arrow). The microvascular network can be seen within the lamina propria; however it is indistinct in comparison to that seen in confocal endomicroscopy images of the small intestine (inset).

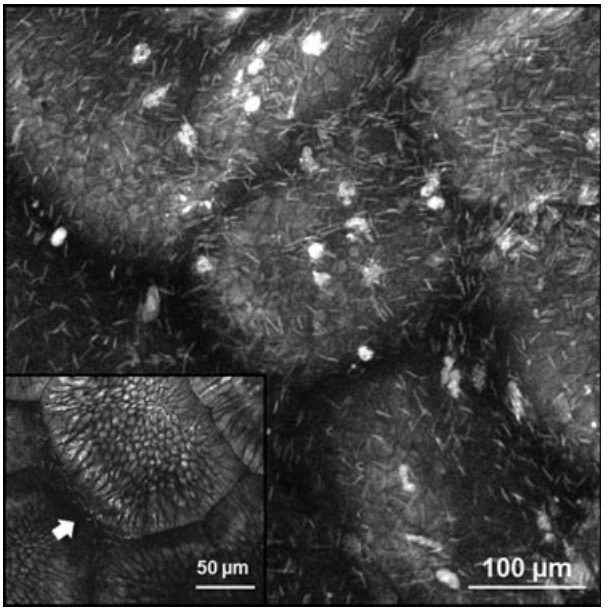

Fig 5. Organisms consistent with *Helicobacter*-like organisms were identified in 13/14 dogs by using confocal endomicroscopy after administration of topical acriflavine and were seen as elongated fluorescent silhouettes displaying a characteristic spiral shape. Organisms were predominantly seen superficially within the gastric mucus, or deeper between gastric folds (inset).

Over the surface of the gastric mucosa, the regular mosaic pattern formed by the epithelial cells was more distinct with acriflavine than fluorescein. Within deeper sections, the nuclei of each individual columnar epithelial cell could be observed forming a regular line against the basement membrane (Fig 3A–C). Despite preferential staining of the nuclei, cytoplasmic detail was also provided, including subcellular detail. For acriflavine, useful imaging was possible to a depth of approximately 50–70 µm, although within the pyloric antrum imaging of the surface epithelial cells, but not the lamina propria, was occasionally possible up to a depth of 100–120 µm where the contrast agent was able to deeply penetrate gastric pits.

Mucosal Changes Identified via CEM and Comparison with Histologic Correlates

In all 13 dogs, organisms consistent with large *Helicobacter*-like organisms (HLOs) were identified by using CEM. These appeared as elongated fluorescent silhouettes displaying a characteristic spiral appearance and were seen both superficially within the gastric mucus as well as within the gastric pits (Fig 5). Histologically, spiral HLOs were identified in standard H&E sections in 11/14 dogs. Organisms were of similar size and shape to that identified on CEM and were predominantly seen superficially between gastric villi, with occasional dense mats of organisms deeper within gastric crypts in some dogs. CEM allowed identification of organisms within the overlying gastric mucus, whereas these were not as readily identified histologically because of loss of mucus during tissue processing. Additional histologic sections stained with WSS confirmed the presence of spiral organisms in all dogs that were positive by using CEM, including the two that were negative with H&E staining. Despite their presence, no appreciable changes that could be directly attributed to the organisms were seen in any of the positive dogs on either histologic sections or with CEM imaging. Lymphoid follicular activation was not identified in any of these dogs.

A number of CEM findings of currently unknown significance were intermittently identified in those dogs that had no identifiable histopathologic changes. In these dogs, isolated cells were seen that demonstrated a distinct difference in fluorescent intensity compared with surrounding cells or that contained vacuoles of variable size within the cytoplasm, or both (Fig 6A).

In 1 dog, infrequently, but wide areas of finely vacuolated cells were identified with retention of the overall surface architecture (Fig 6C). In another, the distinct mosaic pattern of superficial epithelial cells in 1 assessed region was focally disrupted at the very tip of some mucosal folds by cells that had a finely granular appearance to the cytoplasm and occasional cytoplasmic vacuolation (Fig 6B).

Imaging Artifacts

A total of 1,245 CEM images of the gastric mucosa were collected over the course of the first 6 procedures and were each assessed for the presence of artifacts. These 6 procedures were chosen for further evaluation as each had been performed by a single user with one of the CEM endoscopes (GIF-145),

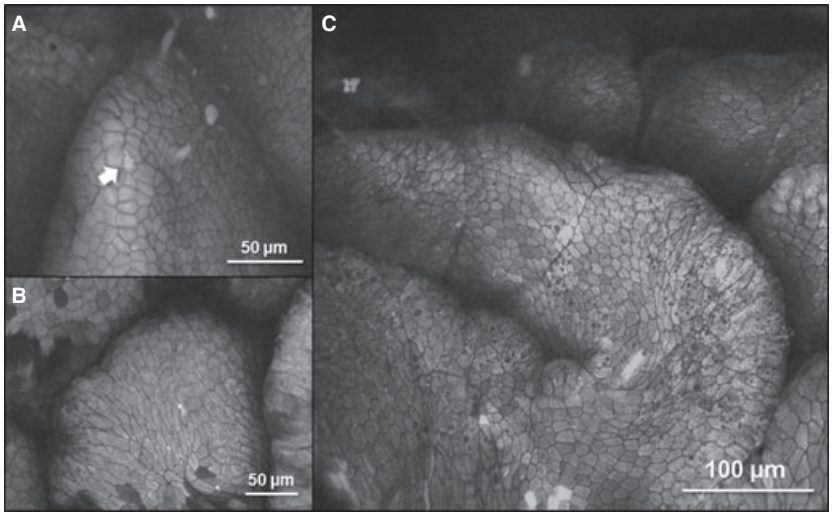

Fig 6. Confocal endomicroscopy identified a number of findings of currently unknown importance. **(A)** Occasional isolated cells demonstrate distinct differences in fluorescent intensity compared with surrounding cells, cytoplasmic vacuolation, or both (arrow). **(B)** The distinct mosaic pattern of the superficial epithelial cells is disrupted in this region, with some cells displaying a finely granular appearance to the cytoplasm. **(C)** In 1 dog, infrequent, but wide areas of finely vacuolated cells were identified. The overall surface architecture was otherwise retained. All images collected after topical acriflavine administration.

whereas the subsequent 8 procedures were performed by a combination of users with the Olympus PCF-Q180AI endoscope.

Image artifact included, but was not limited to, motion artifact, poor mucosal contact, and imaging interference because of luminal debris. Of these, motion artifact was the most common imaging artifact and was observed in 171 of 1,245 (13.7%) images and most commonly occurred secondary to peristalsis (Fig 7A). Despite this, gastric antispasmodic drugs were not required in any of the dogs to facilitate CEM imaging. Slipping of the endoscope tip also contributed to motion artifact and especially occurred where imaging was attempted of surfaces that were not perpendicular to the endoscope tip. The application of suction helped to stabilize contact with the mucosal surface in this circumstance. Although present, motion artifact did not always completely render those images affected uninterpretable as often only a small portion of the image was affected.

Food particles and other superficial debris were occasionally observed in some dogs (Fig 7B). Intermittent and transient obscuring of imaging most commonly resulted, but imaging was still possible. Debris also contributed to poor image resolution when it adhered to the confocal window, but this was generally resolved by wiping the distal tip of the endoscope containing the confocal window across the mucosal surface, or by removing the endoscope for manual cleaning. In 1 dog, however food particulate matter completely obscured imaging of the mucosa and CEM was not possible. In this dog, gross WLE was unremarkable, but microscopic food particles prevented good mucosal contact, and the particulate matter was unable to be adequately removed despite vigorous flushing and the use of suction. In addition, microscopic food particles appeared to limit cellular uptake of acriflavine.

Other imaging artifacts that were also noted included poor mucosal contact resulting in the collection of only partial images, gas bubbles, and occasionally vibration of the optical fiber (Fig 7C and D). Artifacts such as these were resolved either by applying suction, or by breaking and re-establishing contact with the mucosal surface.

With increasing operator experience, both the total number of images acquired during a study and the percentage affected by imaging artifact decreased appreciably. An average of 207.5 images/procedure were collected across the entire 6 procedures evaluated, with motion artifact affecting 80/212 images (37.0%) in procedure 1, compared to 8/131 images (6.1%) in the 6th procedure.

Discussion

Confocal endomicroscopy imaging of the gastric mucosa in dogs is feasible during endoscopy by using the fluorophore protocols described as it is for the small intestine.[14] Images provided are comparable to standard histologic correlates and are available for real-time interpretation during the procedure. Both fluorophore protocols delivered fluorescent contrast and allowed an overall impression of gross mucosal morphology as well as the evaluation of cellular and subcellular features. Fluorescent characteristics of acriflavine and fluorescein were different, thus providing complementary information regarding components of mucosal morphology.

Rapid redistribution of fluorescein from the vascular space to the interstitial and intracellular spaces allowed simultaneous evaluation of cellular detail within the

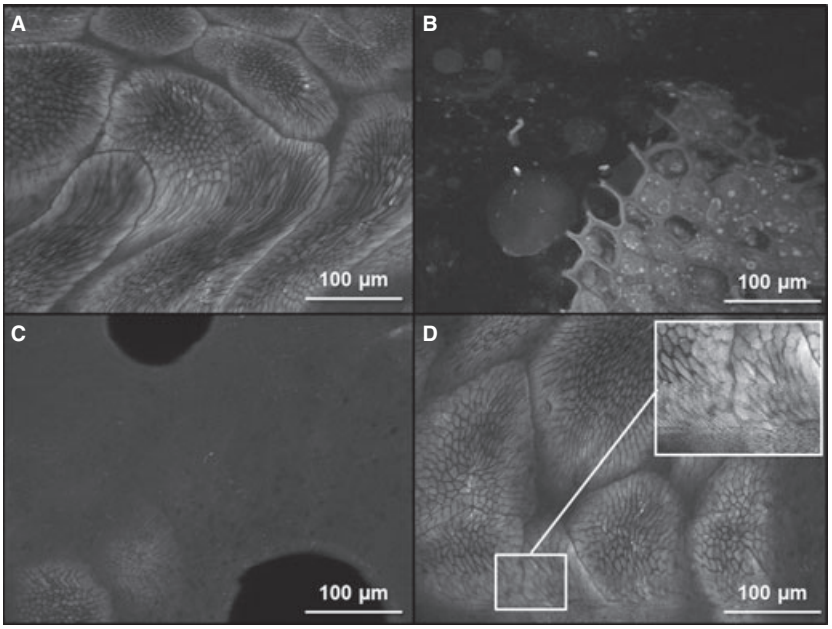

Fig 7. (A) Motion artifact. Confocal endomicroscopy image collected after topical administration of acriflavine demonstrating motion artifact affecting the bottom of the image. **(B) Food particulate matter**. Cellular debris can be seen in the foreground of this image. The sheet of material comprising individual large cell-like structures is consistent with plant material. Image collected after topical administration of acriflavine. **(C) Poor mucosal contact and gas-bubble artifact**. Complete mucosal contact has not been achieved and the mucosal surface is only visualized indistinctly in the bottom left of the image. Large, negatively contrasting, circular artifacts, consistent with gas bubbles are also seen in the upper and lower aspect of the image. Image collected after topical administration of acriflavine. **(D) Vibration artifact**. Vibration of the optical fiber was also occasionally seen as a subtle, but regular, pattern of parallel lines partially obscuring the width of an image (magnified image inset). Image collected after topical administration of acriflavine.

lamina propria and epithelial layers. Uniform distribution throughout the gastric mucosa resulted in predictable fluorescent contrast within each region of the stomach. The assessable depth of the gastric mucosa was superior with fluorescein compared with that achieved with acriflavine. Fluorescein also allowed assessment of the distribution of the microvascular network within the lamina propria, but in comparison to that reported by the authors for the small intestine,[14] precise delineation of the microvascular network and evaluation of blood flow, including passage of individual RBCs, was not possible. A reason for this difference is not clear, but could relate to the depth and distribution of the vasculature within the lamina propria as compared with the small intestine; rapid extravasation of fluorescein; or an overall difference in fluorescent intensity. Each of these could adversely affect both lateral and axial resolution. However, the presence of less distinct vascular features should not be mistaken for an absolute inability to assess the microvascular network. In people, vascular changes including increased focal extravasation of fluorescein, hypervascularity, and irregular short and branching vessels are identifiable by CEM in various gastric disorders.[17–20] Further assessment is required in dogs with disease to determine if similar alteration in the vascular network can be identified.

With fluorescein, imaging was possible for at least 30 minutes, although toward the end of this period higher laser power and image brightness settings were required in order to achieve images of similar resolution. Deterioration in image quality over time after intravenous administration of fluorescein has been demonstrated previously, and was explained as being because of deposition of fluorescent moieties within the tissues contributing to increased signal-to-noise ratio and limiting image resolution.[21]

In contrast, acriflavine was more unpredictable with its fluorescent intensity depending upon the region being assessed, required repeat application for each new area, and had more limited penetration with less consistent uptake in deeper regions of the mucosa. A reason for the differences in fluorescent intensity achieved both between dogs and between different regions of the stomach remains unclear and requires further evaluation, but as fluorescent intensity is reported to be affected by pH, and given that the most consistent contrast was achieved in the pyloric antrum, this might relate to differences in cellular pH among different gastric regions. Alternatively differences in the thickness of overlying gastric mucus could also affect cellular uptake. However, where acriflavine did achieve adequate fluorescent intensity no deterioration in image quality occurred over time. Acriflavine also provided superior subcellular detail including nuclear features, thereby improving identification of individual cells; and in addition allowed detection of gastric HLOs.

Both fluorescein and acriflavine have been routinely used in people undergoing clinical gastrointestinal CEM procedures, however safety concerns regarding potential mutagenic effects of acriflavine have limited its use in humans.[1,4,22] Nuclear features, considered important determinants for differentiating neoplastic versus dysplastic disease, are less apparent with fluorescein although alteration in cytoplasmic distribution is still suggested to assist detection to some degree.

In people, CEM of the gastric mucosa has been used for clinical assessment of a range of gastrointestinal conditions encompassing dysplastic, neoplastic, inflammatory, and autoimmune disease.[1,3,8,10–13] The evaluation of morphologic change to gastric pit patterns in people with various diseases using CEM has permitted development of classification systems that allow both recognition of, and differentiation between, conditions such as atrophic gastritis, chronic inflammatory gastritis, intestinal metaplasia, and even neoplastic diseases including tubular adenocarcinoma.[17] Other CEM changes that have been identified in people include increased lamina propria cellularity corresponding with inflammation or infiltrative neoplasia. Identification of nuclear aberrations or changes in tissue or microvascular architecture via CEM, consistent with or suggestive of neoplastic disease, also helps guide endoscopic biopsy to confirm the presence of disease thereby increasing diagnostic yield.[12,17,23,24] Bacterial translocation, increased epithelial shedding, or alteration in epithelial and vascular permeability with provocative testing with bacterial populations or specific inflammatory cytokines have also been documented with CEM.[25–29] Conjugation of fluorescein isothiocyanate to different molecular weight dextrans facilitates detection of subtle alterations to vascular permeability by aiding retention of the fluorophore within the vascular space.[30,31] These changes might not be able to be evaluated ex vivo or might be significantly affected by tissue processing.

Based upon this study, similar potential exists for disease detection in dogs and a number of cellular and subcellular changes were intermittently recognized in dogs. It is likely that isolated cellular changes are insignificant, but the significance of more widespread change remains unclear and might represent a spectrum of normal; reflect cellular aging and apoptotic change; result from subtle alteration in cellular processes secondary to the presence of HLOS; or be indicative of subclinical disease that was not identified by using standard histologic techniques alone. This requires further exploration in dogs with clinical disease or re-evaluation after eradication of gastric HLOs, but the ability to detect such subtle change possibly indicates an increased potential for CEM technology to detect early gastrointestinal disease.

Correct interpretation of CEM images does however require some investigator experience. Training, by using images with confirmed histopathologic diagnoses, has been shown to be useful to rapidly improve in vivo detection of disease and allow diagnosis by clinical gastroenterologists at the time of the procedure.[9,32–35] Whether the spectrum of diseases typically investigated by veterinary endoscopists lends itself to similar independence from pathologists requires further investigation. One particular initial challenge for interpretation of gastric CEM images is that tissue positioning within confocal images is en face to the mucosal surface, thus providing orthogonal, cross-sectional images compared to the longitudinal tissue sections pathologists would normally interpret (Fig 1, 2A–D). For standard histopathology of endoscopic biopsies this positioning would normally be considered inadequate[16]; however, in comparison to assessing single histologic tissue sections, collection and assessment of multiple optical sections is possible with CEM by successive adjustment of the *z*-axis through a volume of tissue. Furthermore, CEM is not limited by an absolute number of endoscopic biopsies collected and a greater number of sites, as well as a larger region of the gastric mucosa can be assessed. In combination these aspects provide potentially greater diagnostic capability for CEM. This ability to assess an unlimited number of sites does conversely have the potential to greatly extend procedure duration. However, this is not reflected in published reports, nor in the authors' experience where, excluding the initial learning phase, procedure duration was only marginally prolonged compared to that for standard endoscopy alone, with the number of images collected per procedure decreasing with experience.[35] Furthermore, when investigating focal lesions, significant procedure prolongation would be less likely.

The inability to assess deep mucosal and submucosal structures does represent a limitation of current CEM technology. Confocal imaging of gastric crypts in people proves challenging or impossible unless concurrent mucosal atrophy is present, thus making identification of disease affecting these specific regions difficult.[36] Equally, detection of disease in the underlying submucosa is currently impossible via CEM and this could be particularly important for differentiating conditions such as inflammatory bowel disease and lymphoma.[37,38] Adaptation of available technology by utilizing laser light of a higher wavelength could improve tissue penetration and allow for more routine assessment of deeper tissue structures in conjunction with appropriate fluorophores. Further assessment of current CEM technology in dogs with disease is required as deep tissue penetration might not be essential if alternate superficial morphologic changes can be identified that correlate with particular disease. In addition CEM could still improve diagnostic yield, despite a lack of deep tissue penetration, by identifying subtle superficial morphologic changes that aid acquisition of targeted endoscopic biopsies that then allow for histopathologic assessment of deeper structures.

As demonstrated here, the technique of operating the CEM and obtaining usable confocal images presents unique challenges and involved an initial steep learning curve with operation of the endoscope improving with increasing operator experience.[14,33,35]

Both the number of captured images and the percentage affected by artifact reduced as operator experience increased. As operator confidence improved, an overview of a whole region was also more frequently gained by increasing scan rate to assess a larger section of the mucosal surface.

In 1 dog that had been fasted for a standard duration of time, microscopic food particles obscured imaging; limited cellular uptake of the topically administered fluorophore acriflavine, and prevented CEM imaging. This demonstrates the importance of ensuring adequate fasting and might be even more important when assessing dogs with disease, as altered mechanical digestion and delayed gastric emptying might be more likely. Therefore, prolonged fasting could be required.

In conclusion, CEM for evaluation of gastric mucosal morphology is feasible in dogs and provides histologically equivalent images, allowing for real-time assessment during endoscopy. This has implications for aiding in vivo diagnosis of gastrointestinal disease However, further assessment in a larger number of dogs with clinical disease is required before routine clinical use or the development of classification systems can occur.

Footnotes

[a] Olympus Australia, Mt Waverley, Vic., Australia
[b] Optiscan Imaging, Notting Hill, Vic., Australia
[c] ACP 2; Delvet Pty Ltd, Asquith, NSW, Australia
[d] Physeptone; Sigma Pharmaceuticals, Rowville, Vic., Australia
[e] Alfaxan; Jurox Pty Ltd, Rutherford, NSW, Australia
[f] Isorrane; Baxter Healthcare Pty Ltd, Old Toongabbie, NSW, Australia
[g] Sigma Aldrich, Castle Hill, NSW, Australia
[h] Olympus washing catheter (PW-2L-1); Olympus Australia, Mt Waverley, Vic., Australia

Acknowledgments

The study was supported, in part, by grants from the Comparative Gastroenterology Society Waltham's Research grant and by the Victorian Government's Operational Infrastructure Support Program. The confocal endomicroscope was purchased by the University of Melbourne and the Victorian Department of Business and Innovation; Victorian Science Agenda. This equipment forms part of the Victorian Biomedical Imaging Capability.

The authors thank Peter Delaney from Optiscan Imaging for assistance with the initial confocal endomicroscopy procedures; and Dr Julien Dandrieux, Dr Nathalee Prakash, and Dr Anne-Claire Duchaussoy for additional procedural assistance.

Conflict of Interest Declaration: Dr Mellora Sharman and Professor Ted Whittem own minor stock in Optiscan Imaging PTY Ltd.

References

1. Dunbar KB, Canto MI. Confocal endomicroscopy. Tech Gastrointest Endosc 2010;12:90–99.

2. Goetz M, Dunbar K, Canto M. Examination technique of confocal laser endomicroscopy. In: Kiesslich R, Galle PR, Neurath MF, eds. Atlas of Endomicroscopy. Heidelberg: Springer; 2008:25–32.

3. Kiesslich R, Goetz M, Neurath MF. Confocal laser endomicroscopy for gastrointestinal diseases. Gastrointest Endosc Clin N Am 2008;18:451–466.

4. Kiesslich R, Goetz M, Vieth M, et al. Confocal laser endomicroscopy. Gastrointest Endosc Clin N Am 2005;15:715–731.

5. Goetz M, Toermer T, Vieth M, et al. Simultaneous confocal laser endomicroscopy and chromoendoscopy with topical cresyl violet. Gastrointest Endosc 2009;70:959–968.

6. Sharman M, Mansfield C, Whittem T. The exogenous fluorophore, fluorescein, enables in vivo assessment of the gastrointestinal mucosa via confocal endomicroscopy: Optimization of intravenous dosing in the dog model. J Vet Pharmacol Ther 2012;36:450–455.

7. Leong RWL, Chang D, Merrett ND, et al. Taking optical biopsies with confocal endomicroscopy. J Gastroenterol Hepatol 2009;24:1701–1703.

8. De Palma GD. Confocal laser endomicroscopy in the "*in vivo*" histological diagnosis of the gastrointestinal tract. World J Gastroenterol 2009;15:5770–5775.

9. Dunbar KB, Kiesslich R, Deinert K, et al. Confocal laser endomicroscopy image interpretation: Interobserver agreement among gastroenterologists and pathologists. In: Digestive Diseases Week—American Society for Gastrointestinal Endoscopy. Gastrointest Endosc 2007;65(5):AB348.

10. Nguyen NQ, Leong RWL. Current application of confocal endomicroscopy in gastrointestinal disorders. J Gastroenterol Hepatol 2008;23:1483–1491.

11. Kitabatake S, Niwa Y, Miyahara R, et al. Confocal endomicroscopy for the diagnosis of gastric cancer in vivo. Endoscopy 2006;38:1110–1114.

12. Watanabe O, Ando T, Maeda O, et al. Confocal endomicroscopy in patients with ulcerative colitis. J Gastroenterol Hepatol 2008;23:S286–S290.

13. Leong RWL, Nguyen NQ, Meredith CG, et al. In vivo confocal endomicroscopy in the diagnosis and evaluation of celiac disease. Gastroenterology 2008;135:1870–1876.

14. Sharman MJ, Bacci B, Whittem T, et al. *In vivo* confocal endomicroscopy evaluation of small intestinal mucosal morphology in dogs. J Vet Intern Med 2013;27:1372–1378.

15. Sharman MJ, Bacci B, Sutton P, et al. Confocal endomicroscopy enables in vivo identification of gastric *helicobacter*-like organisms in dogs. In: American College of Veterinary Internal Medicine Forum. New Orleans, LA: abstract available in J Vet Intern Med; 2012:26(4):764–765.

16. Washabau RJ, Day MJ, Willard MD, et al. Endoscopic, biopsy, and histopathologic guidelines for the evaluation of gastrointestinal inflammation in companion animals. J Vet Intern Med 2010;24:10–26.

17. Zhang JN, Li Y, Zhao YA, et al. Classification of gastric pit patterns by confocal endomicroscopy. Gastrointest Endosc 2008;67:843–853.

18. Wang P, Ji R, Yu T, et al. Classification of histological severity of *Helicobacter pylori*-associated gastritis by confocal laser endomicroscopy. World J Gastroenterol 2010;16:5203–5210.

19. Liu H, Li Y-Q, Yu T, et al. Confocal endomicroscopy for *in vivo* detection of microvascular architecture in normal and malignant lesions of upper gastrointestinal tract. J Gastroenterol Hepatol 2008;23:56–61.

20. Kakeji K, Yamaguchi S, Yoshida D, et al. Development and assessment of morphologic criteria for diagnosing gastric cancer using confocal endomicroscopy: An ex vivo and in vivo study. Endoscopy 2006;28:886–890.

21. Becker V, von Delius S, Bajbouj M, et al. Intravenous application of fluorescein for confocal laser scanning microscopy: Evaluation of contrast dynamics and image quality with increasing injection-to-imaging time. Gastrointest Endosc 2008;68:319–323.

22. Dunbar K, Canto M. Confocal endomicroscopy. Curr Opin Gastroenterol 2008;24:631–637.

23. Wirths K, Neuhaus H. Endomicroscopy of gastritis and gastric cancer. In: Kiesslich R, Galle PR, Neurath MF, eds. Atlas of Endomicroscopy. Heidelberg: Springer; 2008:60–66.

24. Trovato C, Sonzogni A, Ravizza D, et al. Celiac disease: In vivo diagnosis by confocal endomicroscopy. Gastrointest Endosc 2007;65:1096–1099.

25. Guruge JL, Falk PG, Lorenz RG, et al. Epithelial attachment alters the outcome of *Helicobacter pylori* infection. Proc Nat Acad Sci USA 1998;95(7):3925–3930.

26. Moussata D, Goetz M, Gloeckner A, et al. Confocal laser endomicroscopy is a new imaging modality for recognition of intramucosal bacteria in inflammatory bowel disease in vivo. Gut 2011;60:26–33.

27. Goetz M, Kiesslich R, Neurath MF, et al. Functional and molecular imaging with confocal laser endomicroscopy. In: Kiesslich R, Galle PR, Neurath MF, eds. Atlas of Endomicroscopy. Heidelberg: Springer; 2008:87–92.

28. Moussata D, Goetz M, Watson AJ, et al. In vivo imaging of shedding cells induced by enteral bacteria using confocal endomicroscopy in humans. In: Digestive Diseases Week—American Gastroenterological Association. Gastroenterology 2009;136:(5)A130.

29. Kiesslich R, Goetz M, Angus EM, et al. Identification of epithelial gaps in human small and large intestine by confocal endomicroscopy. Gastroenterology 2007;133:1769–1778.

30. Aychek T, Vandoorne K, Brenner O, et al. Quantitative analysis of intravenously administered contrast media reveals changes in vascular barrier functions in a murine colitis model. Magn Reson Med 2011;66:235–243.

31. Vo LT, Papworth GD, Delaney PM, et al. In vivo mapping of the vascular changes in skin burns of anaesthetised mice by fibre optic confocal imaging (FOCI). J Dermatol Sci 2000;23:46–52.

32. Kiesslich R, Burg J, Vieth M, et al. Confocal laser endoscopy for diagnosing intraepithelial neoplasias and colorectal cancer in vivo. Gastroenterology 2004;127:706–713.

33. Buchner AM, Gomez V, Heckman MG, et al. The learning curve of in vivo probe-based confocal laser endomicroscopy for prediction of colorectal neoplasia. Gastrointest Endosc 2011;73:556–560.

34. Buchner AM, Shahid MW, Wallace AM. The learning curve of probe based CLE for detection of neoplasia in colon polyps. Gastroenterology 2010;138:S95.

35. Neumann H, Vieth M, Atreya R, et al. Prospective evaluation of the learning curve of confocal laser endomicroscopy in patients with IBD. Histol Histopathol 2011;26:867–872.

36. Venkatesh K, Cohen M, Evans C, et al. Feasibility of confocal endomicroscopy in the diagnosis of pediatric gastrointestinal disorders. World J Gastroenterol 2009;15:2214–2219.

37. Evans SE, Bonczynski JJ, Broussard JD, et al. Comparison of endoscopic and full-thickness biopsy specimens for diagnosis of inflammatory bowel disease and alimentary tract lymphoma in cats. J Am Vet Med Assoc 2006;229:1447–1450.

38. Kleinschmidt S, Meneses F, Nolte I, et al. Retrospective study on the diagnostic value of full-thickness biopsies from the stomach and intestines of dogs with chronic gastrointestinal disease symptoms. Vet Pathol 2006;43:1000–1003.

Supporting Information

Additional Supporting Information may be found in the online version of this article:

Video S1. The process of epithelial shedding could occasionally be observed in real time. Images collected after topical administration of acriflavine.